Chemosphere 112 (2014) 248–255

Contents lists available at ScienceDirect

Chemosphere

journal homepage: www.elsevier.com/locate/chemosphere

Molecular control of arsenite-induced apoptosis in *Caenorhabditis elegans*: Roles of insulin-like growth factor-1 signaling pathway

Shunchang Wang [a,*], Xiaoxue Teng [a,b], Yun Wang [a], Han-Qing Yu [c], Xun Luo [a,d], An Xu [d], Lijun Wu [d]

[a] Department of Life Science, Huainan Normal University, Huainan 232001, China
[b] School of Life Sciences, Anhui University, Hefei 230601, China
[c] Department of Chemistry, University of Science & Technology of China, Hefei 230026, China
[d] Key Laboratory of Ion Beam Bioengineering, Hefei Institutes of Physical Science, Chinese Academy of Sciences, Hefei 230031, China

HIGHLIGHTS

- DAF-2, AGE-1 and AKT-1 negatively regulate arsenite-induced apoptosis in *C. elegans*.
- AKT-2 and SGK-1 exerts proapoptotic effects.
- ROS generation is contributed to high levels of apoptotic cells in *daf-16* mutants.
- DAF-16 acts antagonistically on IGF-1 signaling in arsenite-induced apoptosis.

GRAPHICAL ABSTRACT

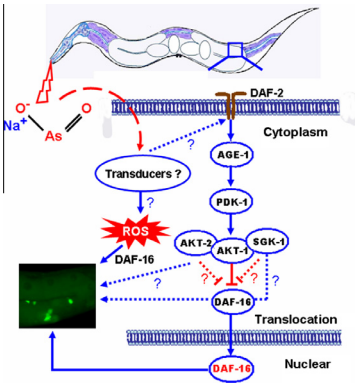

ARTICLE INFO

Article history:
Received 27 December 2013
Received in revised form 2 April 2014
Accepted 5 April 2014
Available online 16 May 2014

Handling Editor: Tamara S. Galloway

Keywords:
Caenorhabditis elegans
Arsenite
Apoptosis
Insulin-like growth factor-1
FOXO
Oxidative stress

ABSTRACT

Apoptosis is one of the main cellular processes in responses to arsenic, the well known environmental carcinogen. By using the nematode *Caenorhabditis elegans* as an *in vivo* model, we found that insulin-like growth factor-1 networks and their target protein DAF-16/FOXO, known as key regulators of energy metabolism and growth, played important roles in arsenite-induced apoptosis. Inactivation of DAF-2, AGE-1 and AKT-1 caused worms more susceptible to arsenite-induced apoptosis, which could be attenuated by DAF-16 knockout. Worms with inactivated AKT-2 and SGK-1 or with constitutively activated PDK-1 and AKT-1 showed low levels of apoptosis, which could be elevated by DAF-16 mutation. Our results demonstrated that DAF-2/IGF-1R, AGE-1/PI3K, PDK-1/PDK1 and AKT-1/PKB negatively regulated the arsenite-induced apoptosis, whereas AKT-2 and SGK-1 acted proapoptotically. DAF-16/FOXO antagonized IGF-1 signals in signaling the arsenite-induced apoptosis, and apoptosis promoted by DAF-16 inactivation was attributed to its higher sensitivity to oxidative stress.

© 2014 Elsevier Ltd. All rights reserved.

1. Introduction

Inorganic arsenic is a well known environmental carcinogen that is up taken by tens of millions of people, mainly from arsenic-rich drinking water (Smith et al., 2000). Chronic exposure to arsenic has been associated with high risks of several cancers, such as cancers of lung, skin, kidney, and liver (Hughes et al., 2011). Depending on cell types, arsenic exposure causes pleiotropic effects. As a tumor promoter, arsenic exposure promotes proliferation and transformation (Ouyang et al., 2008). It can also act as a potent apoptosis inducer that causes apoptosis in many cell lines

* Corresponding author. Tel.: +86 554 666 2817; fax: +86 554 666 3083.
E-mail address: scwangl@hotmail.com (S. Wang).

http://dx.doi.org/10.1016/j.chemosphere.2014.04.021
0045-6535/© 2014 Elsevier Ltd. All rights reserved.

(Ivanov and Hei, 2004; Kumagai and Sumi, 2007). In fact, apoptosis has been considered as one of the main cellular events in response to arsenic exposure (Kumagai and Sumi, 2007). The generation of reactive oxygen species, the induction of genotoxic damages and the disruption of the balance between signal transduction pathways essential for death/survival control are the typically accepted mechanisms for the arsenic-induced apoptosis (Rossman, 2003; Kitchin and Conolly, 2010).

Insulin-like growth factor-1 (IGF-1) signaling networks are well known regulators of energy metabolism and growth. Recent studies have shown that they have promotive roles in tumor progression, mainly through regulation of proliferation, differentiation and apoptosis (Pollak et al., 2004). Increasing evidence suggest that several members of IGF-1 signaling networks are involved in cytotoxic effects of arsenicals (Liu et al., 2006; Hong and Bain, 2012). The IGF-1 signaling is composed of IGF-1 receptor (IGF-1R), phosphoinositide 3-kinase (PI3K), phosphoinositide-dependent kinase-1 (PDK1), AKT/PKB and serum- and glucocorticoid-inducible kinase (SGK) (Párrizas et al., 1997; Pollak et al., 2004). IGF-1R is a membrane-associated tyrosine kinase receptor that transduces diverse extracellular stimuli to PI3K. The activation of PI3K produces a lipid second messenger that is essential for activation of PDK1 and subsequently AKT, which ultimately regulate the activities of Forkhead box class O (FOXO) transcriptional factors (Pollak et al., 2004). FOXO has been found to play pivotal roles in proliferation, apoptosis and stress response (Accili and Arden, 2004; Pinkston-Gosse and Kenyon, 2007). Treatment of human hepatocellular carcinoma cells with As_2O_3 increased the expression of FOXO3a and subsequently nuclear localization, thereby promoted cell cycle arrest and apoptosis (Fei et al., 2009). Since IGF-1 signaling networks and the target protein FOXO have been shown at the center networks of survival and death control, exploration of their roles on arsenite-induced apoptosis is essential for better understanding the cytotoxic/carcinogenetic effects of arsenicals.

The nematode *Caenorhabditis elegans* has been widely used as an emerging model in monitoring environmental toxicants, especially for dissecting key pathways essential for stress response (Leung et al., 2008). Lethality assay showed that *C. elegans* was insensitive to arsenite (Williams and Dusenbery, 1990), however, germline of this animal is subjected to arsenite-induced apoptosis mediated by several conserved signal pathways (Wang et al., 2007; Pei et al., 2008). In *C. elegans,* the evolutionarily conserved IGF-1 signaling is composed of DAF-2/IGF-1R, AGE-1/PI3K and the subsequent PDK-1, AKT-1/2 and SGK-1 (Paradis and Ruvkun, 1998). DAF-16 is the sole homologue of FOXO found in the nematode. Activation of DAF-2 will ultimately repress the activities of DAF-16/FOXO, which regulates several hundreds of genes relating to aging, stress response and germline development (Mukhopadhyay et al., 2006). Recent studies in *C. elegans* have demonstrated that several members of IGF-1 signaling cascades played important roles in apoptosis regulation upon exposing to DNA damage agents (Pinkston-Gosse and Kenyon, 2007; Quevedo et al., 2007). By using *C. elegans* as an *in vivo* model, the main objective of this study was to investigate the roles of IGF-1 signaling pathways and FOXO in arsenite-induced apoptosis.

2. Materials and methods

2.1. Worm strains and chemicals

Strains used in the present study were Bristol N2 wild type, daf-16(mu86) I, daf-16(m26) I, daf-16(mgDf50) I, daf-16(mu86) I; daf-2(e1370) III, daf-16(mgDf47) I; daf-2(e1370) III, zIs356 IV, daf-16(mgDf47) I; xrIs87, daf-16(mg242) I; age-1(mg109) II, age-1(hx546) II, sqt-1(sc13) age-1(mg109)/mnC1 dpy-10(e128) unc-52 II, age-1(mg109) II; akt-1(mg247) V, age-1(mg109) II; pdk-1(mg261) X, sqt-1(sc13) II, daf-2(e1370) III, akt-1(mg144) V, akt-1(ok525) V, akt-2(ok393) X, pdk-1(mg142) X, pdk-1(sa680) X, sgk-1(ok538) X, sgk-1(ft15) X. RNAi feeding strains were purchased from the Source BioScience (Nottingham, UK). L4440 and L453 control vectors were obtained from Addgene (Cambridge, USA). Arsenite ($NaAsO_2$) and Isopropyl-β-D-thiogalactoside (IPTG) were commercial products of Sigma Chemical Inc. (St Louis, USA). Acridine orange (AO) and 5-(and-6)-chloromethyl-2′,7′-dichlorodihydrofluorescein diacetate (CM-H_2DCFDA) were purchased from Molecular Probes (Eugene, USA).

2.2. Worm maintenance and treatment

Worms were cultured at 20 °C in Petri dishes on nematode growth medium (NGM) with a layer of *Escherichia coli* OP50 lawn to serves as food sources. To obtain synchronized worms, gravid hermaphrodites were lysed in alkaline hypochlorite solution. Eggs were collected after lysing and washed three times with M9 buffer. The collected eggs were hatched at 20 °C for 24 h before inoculated onto NGM. The new hatchers arrested at L1 stage without food supply.

Worms were treated using the standard procedures described by Williams and Dusenbery (1990). Briefly, arsenite was diluted to 0.0, 5.0, 10.0, 25.0 μM in K-medium containing *E. coli* OP50 as a food source. For arsenite exposure, 20 synchronized young adult hermaphrodites (20 h post L4 larval) were exposed to graded doses of arsenite in a Costar 12-well tissue plates and cultured at 20 °C for 24 h. For the strain *age-1(mg109)*, worms with left handed roller phenotype were *age-1* null homozygotes and were picked out for arsenite exposure.

2.3. Apoptosis assay

Apoptotic germ cells were scored with a modified AO vital staining as described previously (Shaham, 2006). Briefly, worms were picked from the test wells after 24-h exposure, and transferred into a Costar 24-well plate containing aliquots of 1000 μl M9 buffer supplemented with 25 μg mL^{-1} of AO for each well. To facilitate uptake of the dye, OP50 was added to the buffer prior to staining. Worms were then incubated at 20 °C for 60 min. Animals were allowed to recover for 60 min on bacterial lawns to repel excessive dye in the intestine. Worms were then picked and mounted onto agar pads on microscope slides in 60 μg mL^{-1} levamisole in M9, after which they were examined with an Olympus IX71 inverted microscope (Tokyo, Japan). Pictures were taken using a Zeiss Imager A2 (Jena, Germany) microscope equipped with an AxioCam MRm camera. Only the gonad arm in the posterior part of the body was scored, because the gonad arm near the pharynx was always shaded by intestine.

2.4. ROS determination

ROS were determined as described previously (Gruber et al., 2011). Briefly, 10 age-synchronized worms were transferred to each well of a Costar black 96-well plate containing graded doses of arsenite in 180 μl K-medium. CM-H_2DCFDA was then added to each well at a final concentration of 75 μM. Relative fluorescence intensity was read kinetically under a SpectraMax M2e microplate reader (Sunnyvale, USA) every 10 min for 6 h at 20 °C, using 485 and 535 nm as excitation and emission wavelengths, respectively. ROS was expressed as the average relative fluorescent unit per 10 worms.

2.5. DAF-16 nuclear translocation assay

DAF-16 nuclear translocation was scored by exposing young adult GR1352 worms expressing DAF-16::GFP to graded doses of arsenite, DAF-16::GFP was scored as cytoplasmic or nuclear localization in the anterior part of the body. DAF-16 nuclear translocation were expressed as the percent of worms with DAF-16::GFP nuclear localization. Images were taken with a Zeiss Imager A2 microscope.

2.6. RNAi

RNAi was carried out following the standard procedures (Kamath et al., 2001). Briefly, *E. coli* HT115 (DE3) feeding strains with target genes were picked from streaked plates, they were subsequently inoculated in a 2-ml LB medium supplemented with 100 μg mL^{-1} ampicillin and 12.5 μg mL^{-1} tetracycline. The inocula were cultured overnight at 37 °C. A 20 μl of bacteria was then inoculated into a 2-ml fresh LB containing 100 μg mL^{-1} ampicillin and shook 3 h at 37 °C. To induce double-stranded RNA in the feeding bacteria, aliquots of 150 μl cultures were seeded on NGM agar feeding plates containing 100 μg mL^{-1} ampicillin and 1 mM IPTG, let dry and induce overnight at room temperature. For strain feeding, about 50 synchronized L1 worms were transferred to the feeding plates and allowed to develop to the young adult stage before transferred to test solution. An L4440 vector was used as negative control in RNAi experiments, while an *unc-22* RNAi clone was included in the experiments as a positive control (Estes et al., 2010).

2.7. Data analysis

All values were expressed as means ± standard error, statistical differences ($p < 0.05$) between different concentrations and strains were tested using 2-factor analysis of variance (ANOVA) followed by Tukey's multiple comparison test. Student's *t*-test was performed to compare differences between different strains after RNAi.

3. Results

3.1. Anti-apoptotic effects of DAF-2 and AGE-1

The *C. elegans daf-2* encodes an insulin-like growth factor-1 receptor (IGF-1R) that is known to regulate multiple functions (Kimura et al., 1997). To test whether *daf-2* was involved in arsenite-induced germline apoptosis, worms carrying mutated *daf-2(e1370)* loss-of-function (lf) allele were exposed to graded doses of arsenite. Germ cell corpses were scored by AO vital staining after 24 h of exposure, apoptotic cells showed brilliant green compared to uniformly green of the intact cells in patchytene region (Fig. 1A and B). Compared to N2, worms carrying *daf-2(lf)* allele produced more germ cell corpses (Fig. 1C). The mammalian PI3K homolog *age-1* of *C. elegans* lies downstream of *daf-2*. Upon arsenite exposure, germline apoptosis in *age-1(hx546)* showed no difference compared to N2, while *age-1(mg109)* produced more germ cell corpses than N2 at all doses (Fig. 1D).

3.2. Roles of PDK-1, AKT-1/PKB and SGK-1

The *C. elegans pdk-1* lies downstream of *age-1* and encodes a protein homologous to mammalian 3-phosphoinositide-dependent kinase-1 (PDK1) (Paradis and Ruvkun, 1998). To assess whether *pdk-1* mutation affected germline apoptosis under arsenite exposure, germ cell corpses in *pdk-1(lf)* and *pdk-1(mg142)* gain-of-function (gf) strains at different doses of arsenite were scored. Germ cell corpses in *pdk-1(lf)* strain showed no difference compared to that of N2 at all concentrations. However, apoptotic

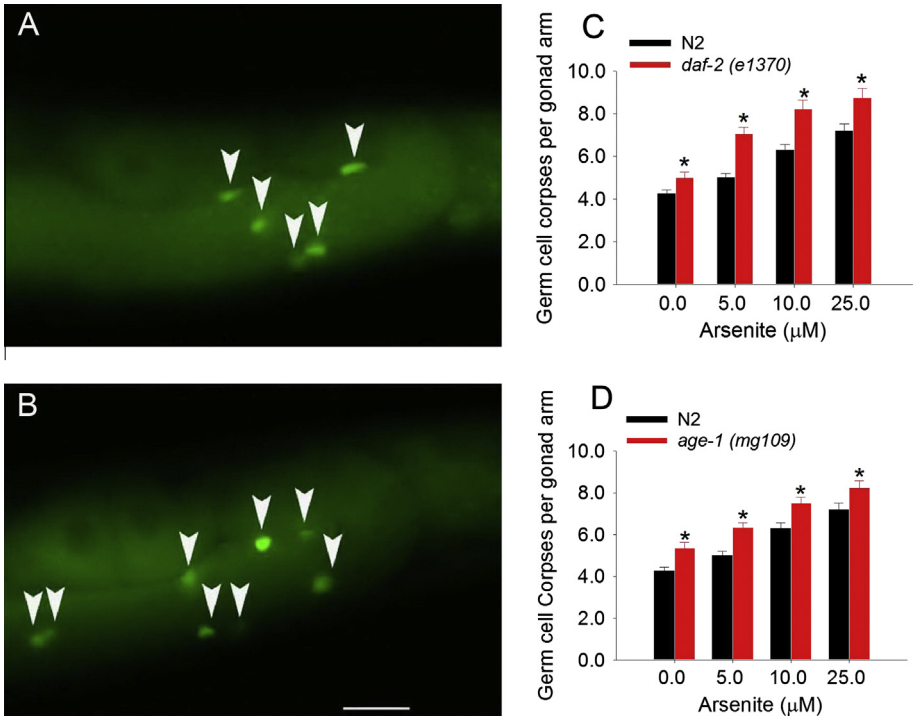

Fig. 1. Arsenite-induced apoptosis in *daf-2* and *age-1* loss-of-function (lf) strains. Representative pictures of germline apoptosis of untreated control (A) and 10 μM (B) of arsenite for 24 h. Germline apoptosis were assayed by acridine orange staining (AO), germ cell corpses were indicated by white arrowheads. The scale bar represents 20 μm. (C) *daf-2 (lf)* caused enhanced germline apoptosis. (D) Germline apoptosis in strains carrying *age-1(lf)* alleles. $^{*}p < 0.05$ represents statistical difference compared to that of N2. For comparison convenience, apoptotic cells for N2 wild type in all figures herein are presented same as those shown in Fig. 1.

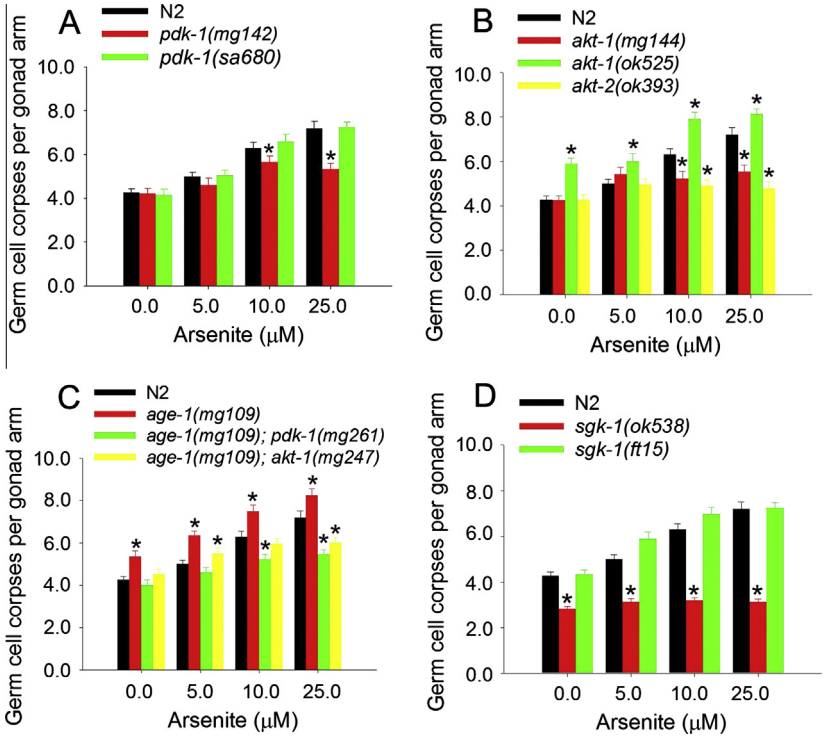

Fig. 2. Roles of *pdk-1*, *akt-1*, *akt-2* and *sgk-1* in arsenite-induced apoptosis. (A) Arsenite-induced apoptosis *pdk-1* mutations. (B) Germline apoptosis in strains with *akt-1* and *akt-2* alleles. (C) Germline apoptosis enhanced by *age-1(mg109)* mutation were suppressed by *akt-1(gf)* and *pdk-1(gf)* mutations. (D) Roles of *sgk-1* in arsenite-induced apoptosis. *pdk(sa680) = pdk-1(lf)*, *pdk-1(mg142) = pdk-1(gf)*, *pdk-1(mg261) = pdk-1(gf)*, *akt-1(ok525) = akt-1(lf)*, *akt-1(mg144) = akt(gf)*, *akt-1(mg247) = akt-1(gf)*, *sgk-1(ok538) = sgk-1(lf)*, *sgk-1(ft15) = sgk-1(gf)*, all of the others were represented as loss-of-function mutations unless otherwise specified.

cells decreased significantly in the strain carrying *pdk-1(gf)* mutation at the doses of 10.0 and 25.0 μM (Fig. 2A). The *C. elegans akt-1* and *akt-2* lie down stream of *pdk-1* (Hertweck et al., 2004). Germ cell corpses per gonad arm in *akt-1(ok525)* lf strain increased dose-dependently compared to N2, while they reduced significantly in *akt-1(mg144)* gf strain at the doses of 10.0 and 25.0 μM (Fig. 2B). For *akt-2(ok393)* lf strain, germ cell corpses per gonad arm were lower than those of N2 at the doses of 10.0 and 25.0 μM (Fig. 2B). The reduction in germline apoptosis was also observed in strains of *age-1(lf)*; *pdk-1(gf)* or *age-1(lf)*; *akt-1(gf)* at the doses of 10.0 and 25.0 μM (Fig. 2C). SGK-1 is a serine/threonine protein kinase that is orthologous to the mammalian serum- and glucocorticoid-inducible kinase (Hertweck et al., 2004). As shown in Fig. 2D, germ cell corpses in *sgk-1(ok538)* lf strain were lower than of N2 physiologically or under arsenite exposure. For *sgk-1(ft15)* gf strain, an enhanced germline apoptosis was observed at the doses of 5.0 and 10.0 μM (Fig. 2D).

3.3. Inactivation of DAF-16/FOXO promoted arsenite-induced apoptosis

The *C. elegans daf-16* encodes a FOXO transcription factor that is governed by the activity of DAF-2 insulin/IGF-1R signaling pathway (Ogg et al., 1997). As shown in Fig. 3A, arsenite-induced apoptosis in N2 and *daf-16(mu86)* lf strain showed no difference at all doses. For mutated alleles of *m26* and *mgDf50*, however, more germ cell corpses per gonad arm were observed at the doses of 5.0 and 10.0 μM respectively. Inactivation of DAF-16 through RNAi also showed high levels of apoptosis at the dose of 10 μM (data not shown). Germ cell corpses showed no difference among all *daf-16* alleles at the elevated doses of 25 μM. Further analysis indicated that DAF-16::GFP rescue transgenetic strains showed inhibitory effects on germline apoptosis at the doses of 10.0 and 25 μM compared to *daf-16* null mutations (Fig. 3B).

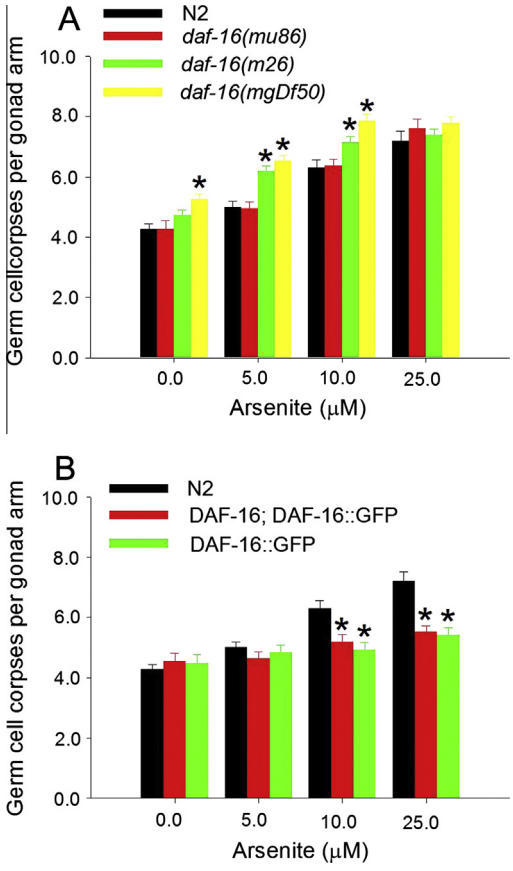

Fig. 3. Roles of *daf-16* in arsenite-induced apoptosis. (A) Worm strains carrying mutated *daf-16* alleles enhanced germline apoptosis dose dependently. (B) DAF-16::GFP transgenetic strains reduced germline apoptosis.

3.4. Antagonistic effects of DAF-16 on IGF-1 signalings

It has been found that phenotypes caused by *daf-2* or *age-1* mutations can be suppressed by *daf-16* mutations (Ogg et al., 1997). To test the antagonistic effect of *daf-16* on arsenite-induced apoptosis, germ cell corpses in strains with *daf-2(e1370); daf-16(mu86)* or *daf-2(e1370); daf-16(mgDf47)* double mutations were scored after 24 h of arsenite exposure. Germ cell corpses in these strains were lower than those of *daf-2(lf)* and higher than those of N2 at the doses of 5.0 and 10.0 μM. At the dose of 25 μM, however, germline apoptosis showed no difference among all strains (Fig. 4A). For *age-1(lf)* mutated strain, *daf-16(lf)* significantly reduced arsenite-induced apoptosis at all doses (Fig. 4B). These results were confirmed by *daf-16* RNAi, which alleviated the levels of apoptosis compared to *daf-2(lf)* or *age-1(lf)* single mutation at the dose of 10 μM (Fig. 4C).

For strain *pdk-1(lf)*, the knockout of *daf-16* through RNAi caused no significant changes in germline apoptosis at the dose of 10 μM. However, *daf-16* RNAi in *pdk-1(gf)* strain produced more germ cell corpses compared to *pdk-1(gf)* single mutation (Fig. 4D). Similar results were found for *akt-1*, in which *daf-16* RNAi in *akt-1(lf)* strain caused no substantial changes in arsenite-induced apoptosis, whereas *daf-16* RNAi in *akt-1(gf)* strain showed a promotive effect (Fig. 4E). Inactivation *daf-16* in *akt-2(lf)* caused a stimulatory effect on germ cell death. For strain *sgk-1(gf)*, germline apoptosis remained unchanged after *daf-16* RNAi, while inactivation of *daf-16* in *sgk-1(lf)* substantially increased arsenite-induced apoptosis (Fig. 4F).

3.5. DAF-16 nuclear translocation

To investigate whether arsenite exposure caused DAF-16 nuclear translocation, we scored the number of worms with DAF-16::GFP nuclear localization after 2 h of arsenite exposure. There were no significant changes in the ratio of DAF-16 nuclear localization at 5.0 and 10.0 μM. At 25 μM or higher dosages, DAF-16::GFP nuclear localization increased dose-dependently (Fig. 5C). It should

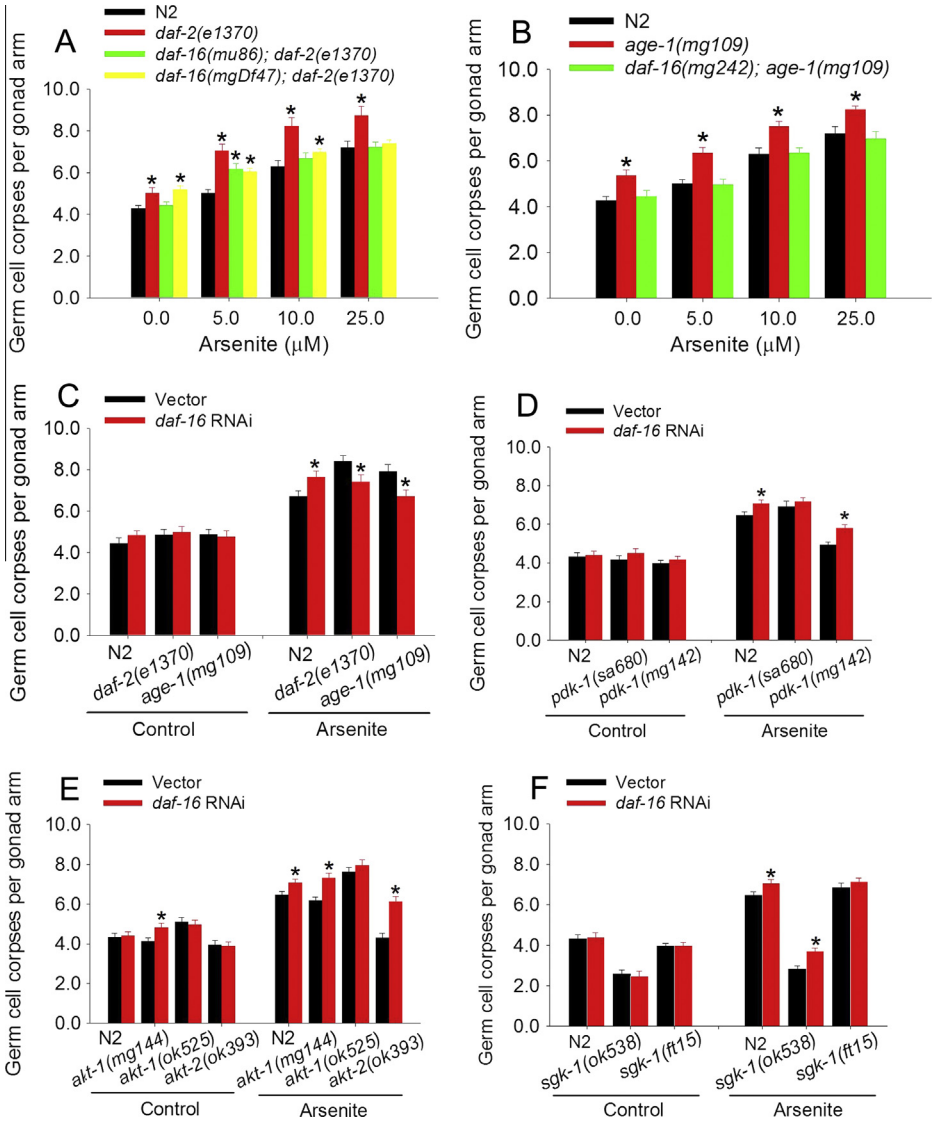

Fig. 4. DAF-16 antagonized IGF-1 signaling in arsenite-induced apoptosis. (A) *daf-16* lf mutations attenuated germline apoptosis in worms with *daf-2(lf)* mutation. (B) *daf-16* lf mutation suppressed arsenite-induced apoptosis enhanced by *age-1(lf)* mutation. (C) *daf-16* RNAi attenuated arsenite-induced apoptosis in *daf-2(lf) or age-1(lf)* strain. (D) Blockage of *daf-16* through RNAi sensitized germline apoptosis in strain with *pdk-1(gf)* allele. (E) Inactivation of *daf-16* increased the sensitivity of arsenite-induced apoptosis in strains with *akt-1(gf)* or *akt-2(lf)* mutation. (F) *daf-16* RNAi enhanced arsenite-induced apoptosis in *sgk-1(gf)* strain.

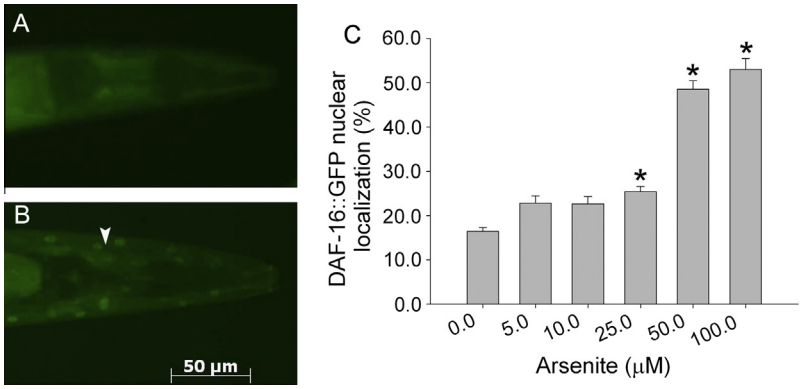

Fig. 5. Arsenite exposure resulted in DAF-16 nuclear translocation. Representative images of cytoplasm DAF-16 localization in untreated control (A) and 25 μM of arsenite (B). DAF-16 translocation was assayed by scoring the ratio of worms with DAF-16::GFP nuclear localization. Images were taken by Zeiss Imager A2 microscope, the scale bar represents 50 μm. (C) Arsenite exposure caused dose-dependent increase in DAF-16 localization. $^{*}p < 0.05$ represents statistical difference compared to untreated control.

be noted that a 24-h prolonged arsenite exposure did not cause any further increase in DAF-16 nuclear localization (data not shown).

3.6. Generation of reactive oxygen species (ROS)

To investigate whether arsenite-induced apoptosis was caused by ROS, different strains of worms were stained with CM-H2DCFDA, and the relative fluorescent units (RFU) were assayed kinetically. As shown in Fig. 6, arsenite exposure caused a dose-dependent increase in average RFU for all strains. Except for *daf-2(lf)*, which presented a low level of ROS compared to N2, no significant differences were observed among all other strains at a given dose of arsenite.

4. Discussion

IGF-1 signaling networks have been shown to play pivotal roles in survival/death control. Recent studies indicated that several members of this signaling were involved in apoptosis regulation in response to arsenicals (Kumagai and Sumi, 2007). The *C. elegans daf-2* is orthologous to mammalian IGF-1R that regulates dauer diapause, aging and stress responses (Kimura et al., 1997; Barsyte et al., 2001). However, the roles of this signal on apoptosis regulation seemed pleiotropic. Inactivation of DAF-2 has been shown to promote germline apoptosis and inhibit gonad tumorous proliferation (Pinkston et al., 2006). However, a recent study showed that *daf-2* promoted germline apoptosis in response to ionized irradiation at 25 °C (Perrin et al., 2013). Our results indicated that *C. elegans* DAF-2/IGF-1R acted as an anti-apoptotic effector in response to arsenite exposure. Activation of PI3K by arsenite has been shown to promote transformation in human HaCaT keratinocytes (Ouyang et al., 2008). Suppression of this signal was linked to enhanced apoptosis induced by arsenic trioxide in B-chronic lymphocytic leukemia (Redondo-Muñoz et al., 2010). Because *age-1(hx546)* was a weak mutation, germline apoptosis in this strain were lower than that of *age-1(mg109)*, the null mutation that caused constitutive dauer diapause. Our data showed that AGE-1/PI3K also acted as an anti-apoptotic effector in response to arsenite exposure. In 3T3-L1 adipocytes, arsenite-induced apoptosis was negatively regulated by PDK1, the homologous of worm PDK-1 (Xue et al., 2011). Unlike DAF-2 or AGE-1, inactivation of PDK-1 did not promote arsenite-induced apoptosis. A possible interpretation is that *pdk-1(sa680)* carries missense mutation and may retain residual activities to its downstream effectors. In fact, as demonstrated in pathogen resistance, signals from DAF-2 may bypass the need for PDK-1 to regulate the activities of DAF-16 (Evans et al., 2008). Since strains of *pdk-1(gf)* or *age-1(lf)*; *pdk-1(gf)* presented less germ cell corpses, PDK-1 was likely to exert anti-apoptotic effects under arsenite exposure.

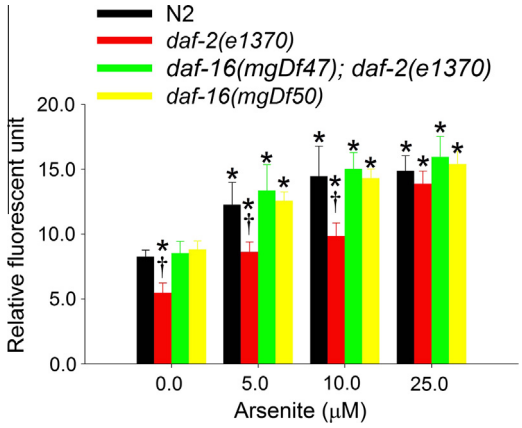

Fig. 6. Arsenite exposure increased the generation of ROS. Worms were exposed to graded doses of arsenite and stained with CM-H_2DCFDA, relative fluorescence intensity (arbitrary unit) were read on a microplate reader kinetically every 10 min for 6 h at 20 °C. *Represents statistical difference ($p < 0.05$) compared to untreated control; †Represents significant difference ($p < 0.05$) between *daf-2(e1370)* and other strains at a given dose of arsenite.

AKT has been reported to be required for human keratinocyte transformation (Ouyang et al., 2008), and the suppression of this signal promoted apoptosis in melanoma cell lines (Rossman, 2003). The *C. elegans* AKT-1 and AKT-2 are candidates to transduce IGF-1 signals in regulation diapause, longevity and stress response (Hertweck et al., 2004). DNA damage-induced apoptosis in *C. elegans* are negatively regulated by AKT-1 and AKT-2 (Quevedo et al., 2007). Like those found in ionized irradiation, activation of AKT-1 protected germline from arsenite-induced apoptosis. AKT-2 is found to function redundantly with AKT-1 to repress dauer formation (Paradis and Ruvkun, 1998). Unexpectedly, inactivation of AKT-2 attenuated arsenite-induced apoptosis, which has not been reported previously. In *C. elegans*, SGK-1 lies paralleled to AKT-1 and AKT-2 that forms a multimeric protein complex in signaling IGF-1 signals in development and stress response (Hertweck et al., 2004). Similar to AKT-2, inactivation of SGK-1 also caused antagonized effects on arsenite-induced apoptosis. In other words, both AKT-2 and SGK-1 played proapoptotic roles in arsenite-induced apoptosis, which were distinct from those of AKT-1 or other members of IGF-1 described above. One reasonable explanation is that strains with mutated *akt-2* or *sgk-1* had small body size and less germ cells in the gonad, thereby presented less germ cell

corpses compared to N2 (Jones et al., 2009; So et al., 2011). It was noteworthy, mitotic cells in strains of *sgk-1(lf)* and *akt-2(lf)* were about 56.8% and 86.6% of N2 under arsenite exposure (data not shown). Another plausible explanation is that AKT-2 and SGK-1 might share distinct phosphorylation patterns with AKT-1 on their target substrate DAF-16, leading to different tissue specificity or different activation patterns. A recent work indicated that AKT-2 and SGK-1 counteracted the function of AKT-1 on gonad development that might cause adverse effects on germline apoptosis (Qi et al., 2012).

In human hepatocellular carcinoma cells, arsenic trioxide increased FOXO3a nuclear localization and subsequently apoptosis promotion (Fei et al., 2009). DAF-16, the only *C. elegans* FOXO homologue, was reported to play anti-apoptotic roles under genotoxic stress (Quevedo et al., 2007). Our results showed that germline apoptosis induced by arsenite was negatively regulated by DAF-16. This result seemed contradictory with other reports, in which DAF-16 protected gonad from tumorous growth through increasing apoptosis (Pinkston et al., 2006; Pinkston-Gosse and Kenyon, 2007). The inconsistent germline apoptosis among different *daf-16* alleles might be caused by mutations in different splicing isoforms (Kwon et al., 2010). In fact, germline apoptosis induced by ionizing radiation also showed discrepant among *daf-16* alleles (Quevedo et al., 2007). The anti-apoptotic effects of DAF-16 might work well at low doses of arsenite, because apoptotic cells at the dose of 25 μM showed no difference among all alleles. To say, the inhibitory effects of DAF-16 on arsenite-induced apoptosis exhibited in a biphasic dose-dependent state. The anti-apoptotic effects of DAF-16 seemed to be strengthened in worms expressing DAF-16::GFP or DAF-16 alpha::GFP::DAF-16B, the transgenetic strains that at least partially rescued *daf-16* mutation, presented less germ cell corpses in response to arsenite. Although DAF-16::GFP or DAF-16 alpha::GFP::DAF-16B has been reported to express in the somatic tissues only, recent studies indicated that ectopic expression DAF-16::GFP affected gonad integrity in worms with *shc-1* mutation (Qi et al., 2012).

DAF-16 is negatively regulated by DAF-2 through AGE-1, PDK-1, AKT-1 and/or SGK-1 cascades (Mukhopadhyay et al., 2006). Under arsenite exposure, worms with either *daf-2* or *daf-16* single mutation showed more susceptible to germline apoptosis. Are there any cooperative or antagonistic effects between DAF-2 and DAF-16 on arsenite-induced apoptosis? As the cases of aging and stress responses, arsenite-induced apoptosis promoted by DAF-2 or AGE-1 dysfunctions were attenuated by DAF-16 depletion. It should be noted, germline apoptosis in worms with *daf-2(e1370) or age-1(mg109)* single mutation were higher than those of *daf-2(e1370); daf-16(lf) or age-1(mg109)*; *daf-16(lf)* double mutations. On the other hand, arsenite-induced apoptosis modulated by IGF-1 signing exhibited in a DAF-16-dependent manner. Furthermore, germline apoptosis in strains of *pdk-1(gf), akt-1(gf), akt-2(lf) and sgk-1(lf)* were enhanced after *daf-16* RNAi. Our results demonstrated that DAF-16 exerted antagonized effects on IGF-1 signaling in response to arsenite-induced apoptosis. However, ablation of *daf-16* by RNAi in *pdk-1(lf)*, *akt-1(lf)* or *sgk-(gf)* strains did not significantly attenuate arsenite-induced apoptosis. Thus, signals from DAF-2 to DAF-16 might bypass PDK-1/AKT-1/2/SGK-1 cascades under arsenite exposure, which are consistent with previous findings (Hertweck et al., 2004).

Although both of DAF-2 and DAF-16 exerted anti-apoptotic effects under arsenite exposure, the underlying mechanisms involved in seemed different. As a transcription factor, DAF-16 exerts its regulatory functions through translocation from cytoplasm to nuclear under reduced IGF-1 signaling or under stress stimuli (Mukhopadhyay et al., 2006). In mammalian, FOXO3a nuclear localization generally leads to either cell cycle arrest or apoptosis (Barsyte et al., 2001; Sakoe et al., 2010). In the absence of IGF-1 signaling, arsenite-induced apoptosis was undoubtedly attributed to the constitutive activation of DAF-16. However, the roles of IGF-1 signaling pathway showed pleiotropic. For example, activation of FOXO3a in MEF cells protects cells from apoptosis mediated by oxidative stress (Mei et al., 2009). With respect to arsenite exposure, DAF-16 nuclear translocation was only observed at the doses exceeding 25 μM. For worms with intact IGF-1/DAF-2 signaling, arsenite-induced apoptosis was unlikely signaled by DAF-16 nuclear localization. It is generally believed that oxidative stress is one of the early events for apoptosis progression under arsenite exposure (Ahmed et al., 2012). FOXO proteins are the key factors in protecting cells from oxidative stress (Accili and Arden, 2004). In *C. elegans*, mutations in *daf-16* increased sensitivities to oxidative stress, and mutation in *daf-2* caused resistance effects (Henis-Korenblit et al., 2004). Therefore, germline apoptosis enhanced by DAF-16 inactivation was ascribed to their hypersensitive to oxidative stress.

In summary, by using *C. elegans* as an *in vivo* model, we demonstrated that IGF-1 signaling component DAF-2/IGF-1R, AGE-1/PI3K, PDK-1 and AKT-1 negatively regulated arsenite-induced apoptosis, while AKT-2 and SGK-1 acted proapoptotically. DAF-16/FOXO exerted antagonistic effects on IGF-1 signals in signaling arsenite-induced apoptosis, and the elevated levels of apoptosis in the absence of DAF-16/FOXO was attributed to their higher sensitivities to oxidative stress.

Acknowledgements

We thank the *Caenorhabditis elegans* Genetics Center, USA, for providing most of the *C. elegans* strains. We would also like to thank the *C. elegans* Gene Knockout Consortium, Canada, for providing some of the mutants. This work was supported by the National Natural Science Foundation of China (21077040), and the Natural Science Foundation of Anhui Province (090413257) and the Scientific Research Foundation of the Higher Education Institutions of Anhui Province (ZD200909).

References

Accili, D., Arden, K.C., 2004. FoxOs at the crossroads of cellular metabolism, differentiation, and transformation. Cell 117, 421–426.

Ahmed, S., Ahsan, K.B., Kippler, M., Mily, A., Wagatsuma, Y., Hoque, A.M., Ngom, P.T., El Arifeen, S., Raqib, R., Vahter, M., 2012. In utero arsenic exposure is associated with impaired thymic function in newborns possibly via oxidative stress and apoptosis. Toxicol. Sci. 129, 305–314.

Barsyte, D., Lovejoy, D.A., Lithgow, G.J., 2001. Longevity and heavy metal resistance in daf-2 and age-1 long-lived mutants of *Caenorhabditis elegans*. FASEB J. 15, 627–634.

Estes, K.A., Dunbar, T.L., Powell, J.R., Ausubel, F.M., Troemel, E.R., 2010. BZIP transcription factor zip-2 mediates an early response to *Pseudomonas aeruginosa* infection in *Caenorhabditis elegans*. Proc. Natl. Acad. Sci. U.S.A. 107, 2153–2158.

Evans, E.A., Chen, W.S., Tan, M.-W., 2008. The DAF-2 insulin-like signaling pathway independently regulates aging and immunity in *C. elegans*. Aging Cell 7, 879–893.

Fei, M., Lu, M., Wang, Y., Zhao, Y., He, S., Gao, S., Ke, Q., Liu, Y., Li, P., Cui, X., Shen, A., Cheng, C., 2009. Arsenic trioxide-induced growth arrest of human hepatocellular carcinoma cells involving FOXO3a expression and localization. Med. Oncol. 26, 178–185.

Gruber, J., Ng, L.F., Fong, S., Wong, Y.T., Koh, S.A., Chen, C.B., Shui, G., Cheong, W.F., Schaffer, S., Wenk, M.R., Halliwell, B., 2011. Mitochondrial changes in ageing *Caenorhabditis elegans* – what do we learn from superoxide dismutase knockouts? PLoS One 6, e19444. http://dx.doi.org/10.1371/journal.pone.0019444.

Henis-Korenblit, S., Zhang, P., Hansen, M., McCormick, M., Lee, S.J., Cary, M., Kenyon, C., 2004. Insulin/IGF-1 signaling mutants reprogram ER stress response regulators to promote longevity. Proc. Natl. Acad. Sci. U.S.A. 2010 (107), 9730–9735.

Hertweck, M., Göbel, C., Baumeister, R., 2004. *C. elegans* SGK-1 is the critical component in the Akt/PKB kinase complex to control stress response and life span. Dev. Cell 6, 577–588.

Hong, G.M., Bain, L.J., 2012. Sodium arsenite represses the expression of myogenin in C2C12 mouse myoblast cells through histone modifications and altered expression of Ezh2, Glp, and Igf-1. Toxicol. Appl. Pharmacol. 260, 250–259.

Hughes, M.F., Beck, B.D., Chen, Y., Lewis, A.S., Thomas, D.J., 2011. Arsenic exposure and toxicology: a historical perspective. Toxicol. Sci. 123, 305–332.
Ivanov, V.N., Hei, T.K., 2004. Arsenite sensitizes human melanomas to apoptosis via tumor necrosis factor alpha-mediated pathway. J. Biol. Chem. 279, 22747–22758.
Jones, K.T., Greer, E.R., Pearce, D., Ashrafi, K., 2009. Rictor/TORC2 regulates *Caenorhabditis elegans* fat storage, body size, and development through sgk-1. PLoS Biol. 7, e1000060.
Kamath, R.K., Martinez-Campos, M., Zipperlen, P., Fraser, A.G., Ahringer, J., 2001. Effectiveness of specific RNA-mediated interference through ingested double-stranded RNA in *C. elegans*. Genome Biol. 2, 1–10.
Kimura, K.D., Tissenbaum, H.A., Liu, Y., Ruvkun, G., 1997. *Daf-2*, an insulin receptor-like gene that regulates longevity and diapause in *Caenorhabditis elegans*. Science 277, 942–946.
Kitchin, K.T., Conolly, R., 2010. Arsenic-induced carcinogenesis–oxidative stress as a possible mode of action and future research needs for more biologically based risk assessment. Chem. Res. Toxicol. 23, 327–335.
Kumagai, Y., Sumi, D., 2007. Arsenic: signal transduction, transcription factor, and biotransformation involved in cellular response and toxicity. Annu. Rev. Pharmacol. Toxicol. 47, 243–262.
Kwon, E.-S., Narasimhan, S.D., Yen, K., Tissenbaum, H.A., 2010. A new DAF-16 isoform regulates longevity. Nature 466, 498–502.
Leung, M.C.K., Williams, P.L., Benedetto, A., Au, C., Helmcke, K.J., Aschner, M., Meyer, J.N., 2008. *Caenorhabditis elegans*: an emerging model in biomedical and environmental toxicology. Toxicol. Sci. 106, 5–28.
Liu, J., Xie, Y., Ducharme, D.M., Shen, J., Diwan, B.A., Merrick, B.A., Grissom, S.F., Tucker, C.J., Paules, R.S., Tennant, R., Waalkes, M.P., 2006. Global gene expression associated with hepatocarcinogenesis in adult male mice induced by in utero arsenic exposure. Environ. Health Perspect. 114, 404–411.
Mei, Y., Zhang, Y., Yamamoto, K., Xie, W., Mak, T.W., You, H., 2009. FOXO3a-dependent regulation of Pink1 (Park6) mediates survival signaling in response to cytokine deprivation. Proc. Natl. Acad. Sci. U.S.A. 106, 5153–5158.
Mukhopadhyay, A., Oh, S.W., Tissenbaum, H.A., 2006. Worming pathways to and from DAF-16/FOXO. Exp. Gerontol. 41, 928–934.
Ogg, S., Paradis, S., Gottlieb, S., Patterson, G.I., Lee, L., Tissenbaum, H.A., Ruvkun, G., 1997. The Fork head transcription factor DAF-16 transduces insulin-like metabolic and longevity signals in *C. elegans*. Nature 389, 994–999.
Ouyang, W., Luo, W., Zhang, D., Jian, J., Ma, Q., Li, J., Shi, X., Chen, J., Gao, J., Huang, C., 2008. PI-3K/Akt pathway-dependent cyclin D1 expression is responsible for arsenite-induced human keratinocyte transformation. Environ. Health Perspect. 116, 1–6.
Paradis, S., Ruvkun, G., 2004. *Caenorhabditis elegans* Akt/PKB transduces insulin receptor-like signals from AGE-1 PI3 kinase to the DAF-16 transcription factor. Genes Dev. 12, 2488–2498.
Párrizas, M., Saltiel, A.R., LeRoith, D., 1997. Insulin-like growth factor 1 inhibits apoptosis using the phosphatidylinositol 3'-kinase and mitogen activated protein kinase pathways. J. Biol. Chem. 1997 (272), 154–161.
Pei, B., Wang, S., Guo, X., Wang, J., Yang, G., Hang, H., Wu, L., 2008. Arsenite-induced germline apoptosis through a MAPK-dependent, p53-independent pathway in *Caenorhabditis elegans*. Chem. Res. Toxicol. 21, 1530–1535.
Perrin, A.J., Gunda, M., Yu, B., Yen, K., Ito, S., Forster, S., Tissenbaum, H.A., Derry, W.B., 2013. Noncanonical control of *C. elegans* germline apoptosis by the insulin/IGF-1 and Ras/MAPK signaling pathways. Cell Death Differ. 20, 97–107.
Pinkston, J.M., Garigan, D., Hansen, M., Kenyon, C., 2006. Mutations that increase the life span of *C. elegans* inhibit tumor growth. Science 313, 971–975.
Pinkston-Gosse, J., Kenyon, C., 2007. DAF-16/FOXO targets genes that regulate tumor growth in *Caenorhabditis elegans*. Nat. Genet. 39, 1403–1409.
Pollak, M.N., Schernhammer, E.S., Hankinson, S.E., 2004. Insulin-like growth factors and neoplasia. Nat. Rev. Cancer 4, 505–518.
Qi, W., Huang, X., Neumann-Haefelin, E., Schulze, E., Baumeister, R., 2012. Cell-nonautonomous signaling of FOXO/DAF-16 to the stem cells of *Caenorhabditis elegans*. PLoS Genet. 8, e1002836.
Quevedo, C., Kaplan, D.R., Derry, W.B., 2007. AKT-1 regulates DNA-damage-induced germline apoptosis in *C. elegans*. Curr. Biol. 17, 286–292.
Redondo-Muñoz, J., Escobar-Díaz, E., Del Cerro, M.H., Pandiella, A., Terol, M.J., García-Marco, J.A., García-Pardo, A., 2010. Induction of B-chronic lymphocytic leukemia cell apoptosis by arsenic trioxide involves suppression of the phosphoinositide 3-kinase/Akt survival pathway via c-jun-NH2 terminal kinase activation and PTEN upregulation. Clin. Cancer Res. 16, 4382–4391.
Rossman, T.G., 2003. Mechanisms of arsenic carcinogenesis. An integrated approach. Mutat. Res. 533, 37–65.
Sakoe, Y., Sakoe, K., Kirito, K., Ozawa, K., Komatsu, N., 2010. FOXO3A as a key molecule for all-trans retinoic acid-induced granulocytic differentiation and apoptosis in acute promyelocytic leukemia. Blood 115, 3787–3795.
Shaham, S., (Ed.), (January 2, 2006). WormBook: Methods in Cell Biology, WormBook, The *C. elegans* Research Community, WormBook, doi/10.1895/wormbook.1.49.1, <http://www.wormbook.org>.
Smith, A.H., Lingas, E.O., Rahman, M., 2000. Contamination of drinking-water by arsenic in Bangladesh: a public health emergency. Bull. World Health Organ. 78, 1093–1103.
So, S., Miyahara, K., Ohshima, Y., 2011. Control of body size in *C. elegans* dependent on food and insulin/IGF-1 signal. Genes Cells 16, 639–651.
Williams, P.L., Dusenbery, D.B., 1990. Aquatic toxicity testing using the nematode *Caenorhabditis elegans*. Environ. Toxicol. Chem. 9, 1285–1290.
Wang, S., Zhao, Y., Wu, L., Tang, M., Su, C., Hei, T.K., Yu, Z., 2007. Induction of germline cell cycle arrest and apoptosis by sodium arsenite in *Caenorhabditis elegans*. Chem. Res. Toxicol. 20, 181–186.
Xue, P., Hou, Y., Zhang, Q., Woods, C.G., Yarborough, K., Liu, H., Sun, G., Andersen, M.E., Pi, J., 2011. Prolonged inorganic arsenite exposure suppresses insulin-stimulated AKT S473 phosphorylation and glucose uptake in 3T3-L1 adipocytes: involvement of the adaptive antioxidant response. Biochem. Biophys. Res. Commun. 407, 360–365.